A model for non-singular black hole collapse and evaporation

Sabine Hossenfelder[1], Leonardo Modesto[2], Isabeau Prémont-Schwarz[2]
[1] *Nordita, Roslagstullsbacken 23, 106 91 Stockholm, Sweden*
[2] *Perimeter Institute for Theoretical Physics, 31 Caroline St.N., Waterloo, ON N2L 2Y5, Canada*

We study the formation of a black hole and its subsequent evaporation in a model employing a minisuperspace approach to loop quantum gravity. In previous work the static solution was obtained and shown to be singularity-free. Here, we examine the more realistic dynamical case by generalizing the static case with help of the Vaidya metric. We track the formation and evolution of trapped surfaces during collapse and evaporation and examine the buildup of quantum gravitationally caused stress-energy preventing the formation of a singularity.

I. INTRODUCTION

The formation of black hole singularities is an inevitable consequence of General Relativity. As instances of infinite energy density and tidal forces, black holes have made headlines, inspired science fiction movies, and were studied in thousands of research articles. It adds to the fascination that we know today black holes are not just a mathematically possible solution to Einstein's field equations, but part of Nature. Since more than a decade now, we have good evidence that our Milky Way, as other galaxies, hosts many stellar black holes as well as a supermassive black hole in its center.

From the perspective of quantum gravity, black holes are of interest because of the infinite curvature towards their center which signals a breakdown of General Relativity. It is an area where effects of quantum gravity are strong, and it is generally expected that these effects prevent the formation of the singularity. Since the black hole emits particles in the process of Hawking radiation [1], the horizon radius decreases. In the standard case it approaches the singularity until both, the singularity and the horizon, vanish in the endpoint of evaporation [2]. However, if the singularity does not exist, this scenario cannot be correct. Since the singularity plays a central role for the causal space-time diagram, its absence in the presence of quantum gravitational effects has consequences for the entire global structure [3], and the removal of the singularity is essential for resolving the black hole information loss problem [4]. To understand the dynamics of the gravitational and matter fields, it is then necessary to have a concrete model.

It is thus promising that it has been shown in a simplified version of loop quantum gravity, known as loop quantum cosmology (LQC) [5], a resolution of singularities, the big bang as well as the black hole singularity [6–8], can be achieved. The regular static black hole metric was recently derived in [9], and studied more closely in [10]. A resolution of the black hole singularity was also obtained in an effective, noncommutative approach to quantum gravity [11] and in asymptotically safe quantum gravity [13]. In another work [12], a 2-dimensional model was used to study the evaporation process in the absence of a singularity.

Here, we will use a 4-dimensional model based on the static solution derived in [9] and generalize it to a dynamical case which then allows us to examine the causal structure. This generalization holds to good accuracy in all realistic scenarios. This approach should be understood not as an exact solution to a problem that requires knowledge of a full theory of quantum gravity, but as a plausible model based on preliminary studies that allows us to investigate the general features of such regular black hole solutions.

Non-singular black holes were considered already by Bardeen in the late 60s and have a long history [14–29]. We will here use a procedure similar to that in [24]. The rest of the paper is organized as follows. We start in the next section by recalling the regular static metric we will be using. In section III we generalize it to a collapse scenario and discuss its properties. In section IV we summarize the thermodynamical properties and, in section V, add the evaporation process and construct the complete causal diagram. The signature of the metric is $(-,+,+,+)$ and we use the unit convention $\hbar = c = G_N = 1$.

II. THE REGULAR SCHWARZSCHILD-METRIC

Let us first summarize the regular black hole metric that we will be using.

Loop Quantum Gravity (LQG) is a candidate theory of quantum gravity. It is obtained from the canonical quantization of the Einstein equations written in terms of the Ashtekar variables [30], that is in terms of an su(2) 3-dimensional connection A and a triad E. The result [31] is that the basis states of LQG are closed graphs the edges of which are labelled by irreducible su(2) representations and the vertices by su(2) intertwiners. Physically, the edges represent quanta of area with area $\gamma l_{\rm P}^2\sqrt{j(j+1)}$, where j is the representation label on the edge (a half-integer), $l_{\rm P}$ is the Planck length, and γ is a parameter of order 1 called the Immerzi parameter. Vertices of the graph represent quanta of 3-volume. The important observation to make here is that area is quantized and the smallest quanta of area possible has area $\sqrt{3}/2\gamma l_{\rm P}^2$.

The regular black hole metric that we will be using is derived from a simplified model of LQG [9]. To obtain

this simplified model we make the following assumptions. First of all, the number of variables is reduced by assuming spherical symmetry. Then, instead of all possible closed graphs, a regular lattice with edge lengths δ_1 and δ_2 is used. The solution is then obtained dynamically inside the homogeneous region (inside the horizon where space is homogeneous but not static). Analytically continuing the solution outside the horizon one finds that one can reduce the two free parameters by imposing that the minimum area present in the solution corresponds to the minimum area of LQG. The one remaining unknown constant δ is a parameter of the model determining the strength of deviations from the classical theory, and would have to be constrained by experiment. With the plausible expectation that the quantum graviational corrections become relevant only when the curvature is in the Planckian regime, corresponding to $\delta < 1$, outside the horizon the solution is the Schwarzschild solution up to negligible Planck-scale corrections which allows us to believe the legitimacy of the analytical extension outside the horizon.

This quantum gravitationally corrected Schwarzschild metric can be expressed in the form

$$ds^2 = -G(r)dt^2 + \frac{dr^2}{F(r)} + H(r)d\Omega \ , \tag{1}$$

with $d\Omega = d\theta^2 + \sin^2\theta d\phi^2$ and

$$\begin{aligned} G(r) &= \frac{(r-r_+)(r-r_-)(r+r_*)^2}{r^4+a_0^2} \ , \\ F(r) &= \frac{(r-r_+)(r-r_-)r^4}{(r+r_*)^2(r^4+a_0^2)} \ , \\ H(r) &= r^2 + \frac{a_0^2}{r^2} \ . \end{aligned} \tag{2}$$

Here, $r_+ = 2m$ and $r_- = 2mP^2$ are the two horizons, and $r_* = \sqrt{r_+ r_-} = 2mP$. P is the polymeric function $P = (\sqrt{1+\epsilon^2}-1)/(\sqrt{1+\epsilon^2}+1)$, with $\epsilon \ll 1$ the product of the Immirzi parameter (γ) and the polymeric parameter (δ). With this, it is also $P \ll 1$, such that r_- and r_* are very close to $r = 0$. The area a_0 is equal to $A_{\min}/8\pi$, $A_{\min}$ being the minimum area gap of LQG.

Note that in the above metric, r is only asymptotically the usual radial coordinate since $g_{\theta\theta}$ is not just r^2. This choice of coordinates however has the advantage of easily revealing the properties of this metric as we will see. But first, most importantly, in the limit $r \to \infty$ the deviations from the Schwarzschild-solution are of order $M\epsilon^2/r$, where M is the usual ADM-mass:

$$\begin{aligned} G(r) &\to 1 - \frac{2M}{r}(1-\epsilon^2) \ , \\ F(r) &\to 1 - \frac{2M}{r} \ , \\ H(r) &\to r^2. \end{aligned} \tag{3}$$

The ADM mass is the mass inferred by an observer at flat asymptotic infinity; it is determined solely by the metric at asymptotic infinity. The parameter m in the solution is related to the mass M by $M = m(1+P)^2$.

If one now makes the coordinate transformation $R = a_0/r$ with the rescaling $\tilde{t} = t\, r_*^2/a_0$, and simultaneously substitutes $R_\pm = a_0/r_\mp$, $R_* = a_0/r_*$ one finds that the metric in the new coordinates has the same form as in the old coordinates and thus exhibits a very compelling type of self-duality with dual radius $r = \sqrt{a_0}$. Looking at the angular part of the metric, one sees that this dual radius corresponds to a minimal possible surface element. It is then also clear that in the limit $r \to 0$, corresponding to $R \to \infty$, the solution does not have a singularity, but instead has another asymptotically flat Schwarzschild region.

The causal diagram for this metric, shown in Fig 1, then has two horizons and two pairs of asymptotically flat regions, A, A' and B, B', as opposed to one such pair in the standard case. In the region enclosed by the horizons, space- and timelikeness is interchanged. The horizon at r_+ is a future horizon for observers in the asymptotically flat B, B' region and a past horizon for observers inside the two horizons. Similarly, the r_- horizon is a future horizon for observers inside the two horizons but a past horizon for observes in A, A'. If one computes the time it takes for a particle to reach $r = 0$, one finds that it takes infinitely long [10]. The diagram shown in Fig 1 is not analytically complete, but should be read as being continued on the dotted horizons at the bottom and top.

The metric in Eq. (2) is a solution of a quantum gravitationally corrected set of equations which, in the absence of quantum corrections $\epsilon, a_0 \to 0$, reproduce Einstein's field equations. However, due to these quantum corrections, the above metric is no longer a vacuum-solution to Einstein's field equations. Instead, if one computes the Einstein-tensor and sets it equal to a source term $G_{\mu\nu} = 8\pi\widetilde{T}_{\mu\nu}$, one obtains an effective quantum gravitational stress-energy-tensor $\widetilde{T}_{\mu\nu}$. The exact expressions for the components of $\widetilde{T}$ are somewhat unsightly and can be found in the appendix. For our purposes it is here sufficient to note that the entries are not positive definite and violate the positive energy condition which is one of the assumptions for the singularity theorems.

III. COLLAPSE

We will proceed by combining the static metric with a radially ingoing null-dust, such that we obtain a dynamical space-time for a black hole formed from such dust. Usually described by the Vaidya metric [32], we will in this scenario have corrections to the Vaidya metric that are negligible in the asymptotic region, but avoid the formation of a singularity in the strong-curvature region. The metric constructed this way in the following is not a strict solution of the minusuperspace LQC equations. However, as long as the null-dust does not already display strong quantum gravitational effects by its mass profile,

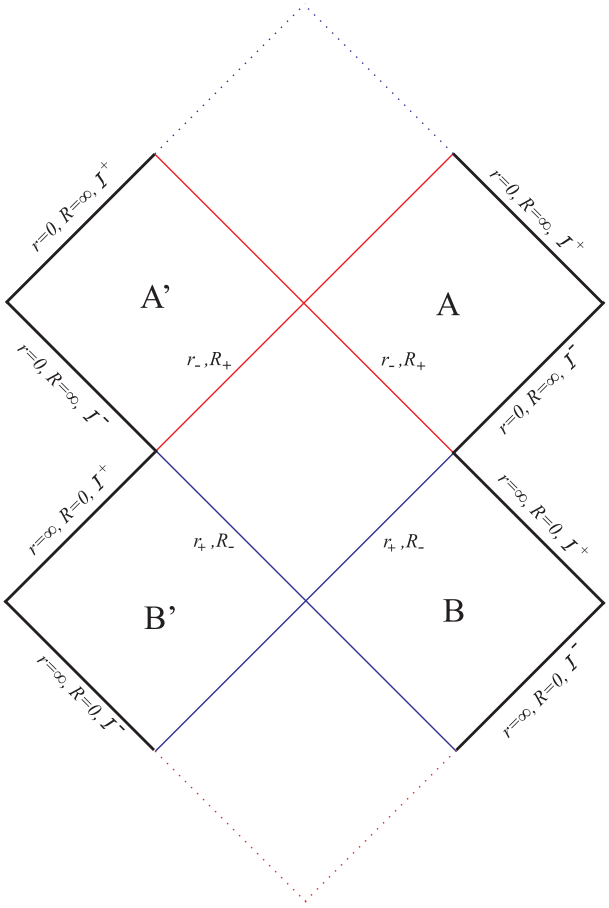

FIG. 1. Penrose diagram of the regular static black hole solution with two asymptotically flat regions. The both horizons, located at r_+ and r_-, are marked in blue and red respectively.

this solution should hold to good accuracy[1].

We start by making a coordinate transformation and rewrite the static space-time in terms of the ingoing null-coordinate v. It is defined by the relation $dv = dt + dr/\sqrt{F(r)G(r)}$, which can be solved to obtain an explicit expression for v. The metric then takes the form

$$ds^2 = -G(r)dv^2 + 2\sqrt{\frac{G(r)}{F(r)}}\,drdv + H(r)d\Omega^2 \,. \quad (4)$$

Now we allow the mass m in the static solution to depend on the advanced time, $m \to m(v)$. Thereby, we will assume the mass is zero before an initial value v_a and that the mass stops increasing at v_b. We can then, as before, use the Einstein equations $G = 8\pi\widetilde{T}$ to obtain the effective quantum gravitational stress-energy tensor

[1] It has been claimed in [33] that, counterintuitively, quantum gravitational effects could become important already at the horizon when the collapse proceeds slowly. However, since we are considering null-dust, the collapse is as fast as can possibly be and these considerations do not apply.

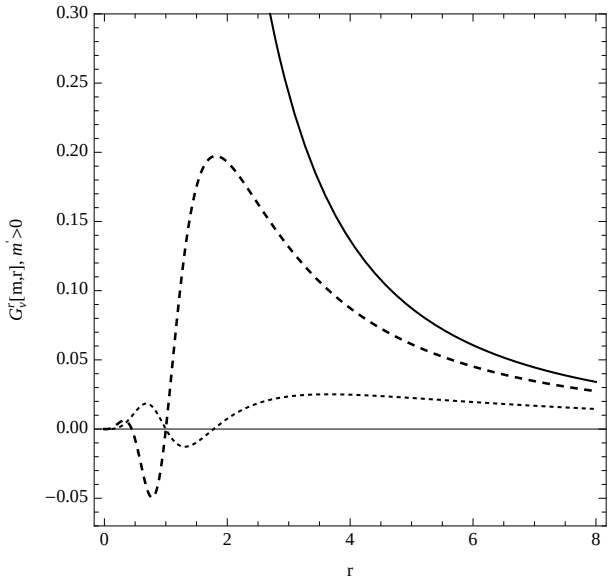

FIG. 2. $G^r{}_v$ as a function of r for radially ingoing radiation and $m'(v) = 1$. The solid line depicts the classical case for $\epsilon, a_0 \to 0$. The long dashed line is for $m(v) = 20$, $(r_* > \sqrt{a_0})$ and the short dashed line is for $m(v) = 5$, $(r_* < \sqrt{a_0})$. All quantities are in Planck units.

$\widetilde{T}$. $\widetilde{T}^v_v$ and $\widetilde{T}^r_r$ do not change when $m(v)$ is no longer constant. The transverse pressure $\widetilde{T}^\theta_\theta = \widetilde{T}^\phi_\phi$ however has an additional term

$$\widetilde{T}^\theta_\theta(m(v)) = \widetilde{T}^\theta_\theta(m) - \frac{Pr^2m'(v)}{2\pi(r+2m(v)P)^4} \,, \quad (5)$$

where $m' = dm/dv$. Because of the ingoing radiation, the stress-energy-tensor now also has an additional non-zero component, $\widetilde{T}^r_v$, which describes radially ingoing energy flux

$$G^r{}_v = \frac{2(1+P)^2r^4(r^4-a_0^2)(r-r_*(v))m'(v)}{(a_0^2+r^4)^2(r+r_*(v))^3} \,. \quad (6)$$

Notice that also in the dynamical case, trapping horizons still occur where $g^{rr} = F(r,v)$ vanishes [34, 35], so we can continue to use the notation from the static case just that $r_\pm(v)$ and $r_*(v)$ are now functions of v. The r-dependence of this component is depicted in Fig 2.

This metric reduces to the Vaidya solutions at large radius, or for $\epsilon \to 0, a_0 \to 0$. However, in the usual Vaidya solutions, the ingoing radiation creates a central singularity. But as we see here, with the quantum gravitational correction, the center remains regular.

We note that the ingoing energy flux has two zeros, one at $r = r_*(v)$ and one at $r = \sqrt{a_0}$, and is negative between these. What happens is that the quantum gravitational correction works against the ingoing flux by making a negative contribution until the effective flux has dropped to zero at whatever is larger, the horizon's geometric mean r_* or the location of the dual radius $r = \sqrt{a_0}$. The flux then remains dominated by the quantum gravitational effects, avoiding a collapse, until it has passed

r_* and the dual radius where it quickly approaches what looks like an outgoing energy flux to the observer in the second asymptotic region.

Since in the second asymptotic region A, A' the mass assigned to the white hole is inversely proportional to the ADM mass at $r = \infty$, the white hole's mass must be decreasing, consistent with the outgoing (or rather through-falling) energy flux. In this process, the past horizon will move towards smaller R or larger r, respectively.

IV. THERMODYNAMICS

Let us now briefly summarize the findings about the thermodynamical properties of this black hole solution, discussed in more detail in [10].

Particle creation can take place at the horizons r_+ and r_- where there is high blueshift when tracing back light-rays. However, if the vacuum at $\mathcal{I}^-$ in the black hole's asymptotic region B, B' is empty of particles as usual, then there will be no flux from particle creation at r_- to $\mathcal{I}^+$ in the second asymptotic region A, A'. This is a consequence of causality and energy conservation, which we can see as follows.

Consider there was a particle creation at r_- resulting in a flux of Hawking radiation towards $R = \infty$. The background is the time-reversed black hole situation but the flux is not time-reversed. This would mean a decrease of the white hole's mass for the observer at $R = \infty$. However, since our metric is geodesically complete, the particles emitted at the white hole's horizon r_- can be traced back all the way to $\mathcal{I}^-$ in the black hole's asymptotic region B, B'. We recall that the white hole's mass for the observer in the A, A' region is inversely proportional to the black hole's mass and see that this particle creation at r_- would contribute to an increase of the black hole's mass corresponding to the decrease of the white hole's mass. Since there is particle emission also at the other horizon r_+, we would have to add both fluxes to obtain the net mass change.

However, we do as usual have a choice for the initial vacuum state at $\mathcal{I}^-$ and we will assume as normally that the vacuum in the black hole's asymptotic past is empty. From the above explanation we see now that this can only be the case if there is no particle flux from r_- to the white hole's asymptotic region $\mathcal{I}^+$. To achieve this, we have to chose the vacuum at $\mathcal{I}^-$ in the white hole's asymptotic region A, A' such that it contains a constant flux into the white hole with the effect that there is no outgoing particle flux created at r_-. This is the time-reversed situation of an evaporating black hole with an empty ingoing vacuum. This situation is mathematically consistent because particle production in the curved background only tells us the relation between the ingoing and outgoing vacuum states, but not the vacuum states themselves. We thus chose the vacuum state at $\mathcal{I}^-$ in the white hole's asymptotic region A, A' such that at r_- there is no additional outgoing flux created [2].

Thus, the evaporation proceeds through the Hawking emission at r_+, and the black hole's Bekenstein-Hawking temperature, given in terms of the surface gravity κ by $T_{BH} = \kappa/2\pi$, yields [10]

$$T_{BH}(m) = \frac{(2m)^3(1-P^2)}{4\pi[(2m)^4 + a_0^2]} \ . \tag{7}$$

This temperature coincides with the Hawking temperature in the limit of large masses but goes to zero for $m \to 0$.

The luminosity can be estimated by use of the Stefan-Boltzmann law $L(m) = \alpha A_H(m) T_{BH}^4(m)$, where (for a single massless field with two degrees of freedom) $\alpha = \pi^2/60$, and $A_H(m) = 4\pi[(2m)^2 + a_0^2/(2m)^2]$ is the surface area of the horizon. Inserting the temperature, we obtain

$$L(m) = \frac{16\, m^{10} \alpha\, (1-P^2)^4}{\pi^3 (a_0^2 + 16\, m^4)^3} \ . \tag{8}$$

The mass loss of the black hole is given by $-L(m)$,

$$\frac{dm(v)}{dv} = -L[m(v)] \tag{9}$$

and we can integrate its inverse to obtain the mass function $m(v)$. The result of this integration with initial condition $m(v=0) = m_0$ is

$$\begin{aligned} v = &\frac{5a_0^6 + 432 a_0^4 m^4 + 34560 a_0^2 m^8 - 61440 m^{12})\pi^3}{720 m^9 (1-P^2)^4 \alpha} \\ &- \frac{5a_0^6 + 432 a_0^4 m_0^4 + 34560 a_0^2 m_0^8 - 61440 m_0^{12})\pi^3}{720 m_0^9 (1-P^2)^4 \alpha} \ . \end{aligned} \tag{10}$$

In the limit $m \to 0$ this expression becomes $v \approx a_0^6 \pi^3/(144 m^9 (1-P^2)^4 \alpha)$, and one thus concludes that the black hole needs an infinite amount of time to completely evaporate.

V. COLLAPSE AND EVAPORATION

We are now well prepared to combine formation and evaporation of the black hole. As in section III, we divide space-time into regions of advanced time. We start with empty space before v_a, let the mass increase from v_a to v_b, and stop the increase thereafter. Hawking radiation will set in, but for astrophysical black holes this evaporation will proceed very slowly, such that we have a long time span during which the black hole is quasi-stable and m remains constant to good accuracy at m_0. Then, at some later time, v_c, Hawking radiation becomes relevant and

[2] Alternatively, we could demand the vacuum at past infinity in the second asymptotic region to be free of particles, but then the vacuum in the black hole region's past infinity would have to contain particles. We will not further consider this possibility here.

m decreases until it reaches zero again. As we have seen in the previous section, it will reach zero only in the limit $v \to \infty$.

We thus have the partition $-\infty < v_a < v_b < v_c < \infty$ with

$$\forall v \in (-\infty, v_a) : m(v) = 0, \tag{11}$$
$$\forall v \in (v_a, v_b) : d/dv\ m(v) > 0, \tag{12}$$
$$\forall v \in (v_b, v_c) : m(v) = m_0, \tag{13}$$
$$\forall v \in (v_c, +\infty) : d/dv\ m(v) < 0, \tag{14}$$
$$\text{for } v \to +\infty : m(v) \to 0. \tag{15}$$

Strictly speaking the mass would immediately start dropping without incoming energy flux and thus $v_a = v_b$, but stretching this region out will be more illuminating to clearly depict the long time during which the hole is quasistable.

To describe the Hawking-radiation we will consider the creation of (massless) particles on the horizon such that locally energy is conserved. We then have an ingoing radiation with negative energy balanced by outgoing radiation of positive energy. Both fluxes originate at the horizon and have the same mass profile which is given by the Hawking temperature. The area with ingoing negative density is again described by an ingoing Vaidya solution, while the one with outgoing positive density is described by an outgoing Vaidya solution.

The outgoing Vaidya solution has a mass-profile that depends on the retarded time u instead of v and the mass decreases instead of increases. The retarded time is defined by $du = dt - dr/\sqrt{F(r)G(r)}$. After a coordinate transformation, the metric reads

$$ds^2 = -G(r,u)du^2 - 2\sqrt{\frac{G(r,u)}{F(r,u)}}dudr + H(r)d\Omega\ , \tag{16}$$

where $F(r,u)$ and $G(r,u)$ have the same form as in the static case (2), but with where m is replaced by a function $m(u)$. We fix the zero point of the retarded time u so that $r = r_+$ corresponds to $u_c = v_c$. Then there is a static region with total mass m_0 for $v > v_c$, $u < u_c$. Note that since the spacetime described here has neither a singularity nor an event horizon, we can consider pair creation to happen directly at the trapping horizon instead of at a different timelike hypersurface outside the horizon, as done in [36]. We have in this way further partitioned spacetime in regions, broken down by retarded time:

$$\forall u < u_c : m(u) = m_0\ , \tag{17}$$
$$\forall u > u_c : d/du\ m(u) < 0\ . \tag{18}$$

Now that we have all parts together, let us explain the complete dynamics as depicted in the resulting causal diagram Fig.3.

In the region $v < v_a$ we have a flat and empty region, described by a piece of Minkowski-space. For all times $v > v_a$, the inner and outer trapping horizons are present.

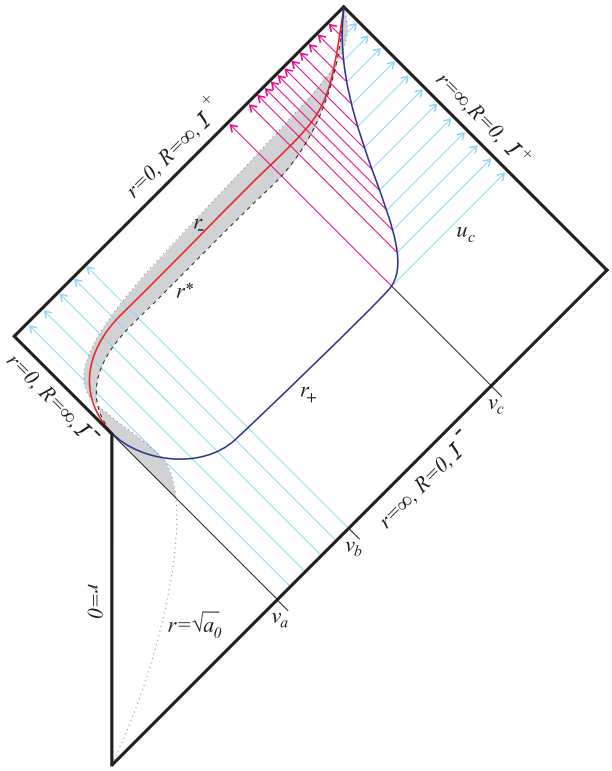

FIG. 3. Penrose diagram for the formation and evaporation of the regular black hole metric. The red and dark blue solid lines depict the two trapping horizons r_- and r_+. The brown, dotted line is the curve of $r = \sqrt{a_0}$ and the black, short dashed one is r_*. The light blue arrows represent positive energy flux, the magenta arrows negative energy flux.

These horizons join smoothly at $r = 0$ in an infinite time and enclose a non-compact region of trapped surfaces.

A black hole begins to form at $v = v_a$ from null dust which has collapsed completely at $v = v_b$ to a static state with mass m_0. It begins to evaporate at $v = v_c$, and the complete evaporation takes an infinite amount of time. The observer at $\mathcal{I}^+$ sees particle emission set in at some retarded time u_c which corresponds to the lightlike surface where the horizon has lingered for a long time. The region with $v > v_c$ is then divided into a static region for $u < u_c$, and the dynamic Vaidya region for $u > u_c$, which is further subdivided into an ingoing and an outgoing part.

As previously mentioned, the radially ingoing flux (light blue arrows) in the collapse region is not positive everywhere due to the quantum gravitational contribution. It has a flipped sign in the area between r_* (black short dashed curve) and $r = \sqrt{a_0}$ (brown dotted curve) which is grey shaded in the figure. Likewise, the ingoing negative flux during evaporation (magenta arrows) has another such region with flipped sign. It is in this region, between the two horizon's geometric mean value r_* and the dual radius corresponding to the minimal area, that the quantum gravitational corrections noticeably modify the classical and semi-classical case, first by preventing

the formation of a singularity, and then by decreasing the black hole's temperature towards zero.

VI. CONCLUSIONS

We have investigated a model for collapse and evaporation of a black hole that is entirely singularity-free. The spacetime does not have an event horizon, but two trapping horizons. By generalizing the previously derived static metric to a dynamical one by use of the Vaidya metric we found that the gravitational stress-energy tensor builds up a negative contribution that violates the positive energy condition and prevents the formation of a singularity. We divided spacetime into six different regions described by different metrics, and constructed the causal diagram for the complete evaporation. The value of the scenario studied here is that it provides a concrete, calculable, model for how quantum gravitational effects alter the black hole spacetime.

ACKNOWLEDGEMENTS

LM is extremely grateful for the fantastic environment offered by Perimeter Institute. Research at Perimeter Institute is supported by the Government of Canada through Industry Canada and by the Province of Ontario through the Ministry of Research & Innovation.

APPENDIX

The effective energy momentum tensor is defined by $\widetilde{T}^{\mu}_{\nu} = G^{\mu}_{\ \nu}/8\pi$. The components of the Einstein tensor in coordinate (v, r, θ, φ) are:

$$
\begin{aligned}
G^{v}_{\ v} &= \frac{r^2}{(a_0^2+r^4)^3(r+r_*)^3} \times \\
&[2a_0^2r^4(r+r_*)(6r^2+7r_-r_+-7r(r_-+r_+)-2rr_* \\
&-r_*^2)-a_0^4(-r_-r_+r_*+r_*^3+2r^2(r_-+r_++2r_*) \\
&+3r(-r_-r_++r_*^2))-r^8(-r_-r_+r_*+r_*^3 \\
&+r(r_-r_++2(r_-+r_+)r_*+3r_*^2))] \ , \\
G^{r}_{\ r} &= -\frac{r^2}{(a_0^2+r^4)^3(r+r_*)^3} \times \\
&[2a_0^2r^4(r+r_*)(-r_-r_++r_*^2+r(r_-+r_++2r_*)) \\
&+a_0^4(4r^3-2r^2(r_-+r_+-2r_*)-r_-r_+r_*+r_*^3 \\
&+r(r_-r_++3r_*^2))+r^8(4r^2r_*+3r_-r_+r_*+r_*^3 \\
&+r(r_-r_+-2(r_-+r_+)r_*+3r_*^2))] \ , \\
G^{\theta}_{\ \theta} &= \frac{r^3}{(a_0^2+r^4)^3(r+r_*)^4} \times \\
&[r^7(r^2r_-r_++r(2r^2+6r_-r_+-3r(r_-+r_+))r_* \\
&+(r-2r_-)(r-2r_+)r_*^2)+2a_0^2r^4(r^2(r_-+r_+) \\
&+(r_-+r_+)r_*^2+r(r_--r_*)(-r_++r_*)) \\
&+a_0^4(4r^3-2r^2(r_-+r_+-3r_*)+2r_-r_+r_* \\
&+r(r_-r_+-3(r_-+r_+)r_*+r_*^2))] \ . \qquad (19)
\end{aligned}
$$

[1] S. W. Hawking, Comm. Math. Phys. **43**, 199 (1975).
[2] S. W. Hawking, Phys. Rev. **D14**, 2460 (1976).
[3] A. Ashtekar and M. Bojowald, Class. Quantum Grav. **22**, 3349 (2005) [arXiv:gr-qc/0504029].
[4] S. Hossenfelder and L. Smolin, arXiv:0901.3156 [gr-qc].
[5] M. Bojowald, Living Rev. Rel. **8**, 11 (2005) [arXiv:gr-qc/0601085].
[6] A. Ashtekar and M. Bojowald, Class. Quant. Grav. **23**, 391 (2006) [arXiv:gr-qc/0509075].
[7] L. Modesto, Phys. Rev. D **70** 124009 (2004), [gr-qc/0407097].
[8] L. Modesto, Class. Quant. Grav. **23**, 5587 (2006) [arXiv:gr-qc/0509078].
[9] L. Modesto, [arXiv:0811.2196 [gr-qc]].
[10] L. Modesto and I. Premont-Schwarz, Phys. Rev. D **80**, 064041 (2009) [arXiv:0905.3170 [hep-th]].
[11] P. Nicolini, A. Smailagic and E. Spallucci, Phys. Lett. B **632**, 547 (2006).
[12] A. Ashtekar, V. Taveras and M. Varadarajan, Phys. Rev. Lett. **100**, 211302 (2008) [arXiv:0801.1811 [Unknown]].
[13] M. Reuter, A. Bonanno, Phys. Rev. D **62**, 043008 (2000) [hep-th/0002196]; Phys. Rev. D **73**, 083005 (2006) [hep-th/0602159].
[14] J. Bardeen, Proc. GR5, Tiflis, USSR (1968).
[15] V. P. Frolov, M. A. Markov and V. F. Mukhanov, Phys. Lett. B **216**, 272 (1989).
[16] V. P. Frolov, M. A. Markov and V. F. Mukhanov, Phys. Rev. D **41**, 383 (1990).
[17] R. Balbinot and E. Poisson, Phys. Rev. D **41**, 395 (1990).
[18] A. Aurilia, R. Balbinot and E. Spallucci, Phys. Lett. B **262**, 222 (1991).
[19] I. Dymnikova, Gen. Rel. Grav. **24**, 235 (1992); Int. J. Mod. Phys. **D5**, 529 (1996); Class. Quantum Grav. **19**, 725 (2002); Int. J. Mod. Phys. **D12**, 1015 (2003).
[20] M. Mars, M. M. Martín-Prats and J. M. M. Senovilla, Class. Quantum Grav. **13**, L51 (1996).
[21] A. Borde, Phys. Rev. **D55**, 7615 (1997).
[22] E. Ayón-Beato and A. Garciá, Phys. Rev. Lett. **80**, 5056 (1998).
[23] M. R. Mbonye and D. Kazanas, Phys. Rev. **D72**, 024016 (2005).

[24] S. A. Hayward, Phys. Rev. Lett. **96**, 031103 (2006) [arXiv:gr-qc/0506126].
[25] P. Nicolini, J. Phys. A **38**, L631 (2005).
[26] S. Ansoldi, P. Nicolini, A. Smailagic and E. Spallucci, Phys. Lett. B **645**, 261 (2007).
[27] E. Spallucci, A. Smailagic and P. Nicolini, holes," Phys. Lett. B **670**, 449 (2009).
[28] P. Nicolini and E. Spallucci, holes," arXiv:0902.4654 [gr-qc].
[29] P. Nicolini, Int. J. Mod. Phys. A **24**, 1229 (2009).
[30] A. Ashtekar, Phys. Rev. Lett. **57** (18): 22442247 (1986).
[31] S. Mercuri, arXiv:1001.1330 [gr-qc].
[32] P. C. Vaidya, Proc. Indian Acad. Sci. **A33**, 264 (1951).
[33] C. Barcelo, S. Liberati, S. Sonego and M. Visser, Phys. Rev. D **77**, 044032 (2008) [arXiv:0712.1130 [gr-qc]].
[34] S. A. Hayward, Phys. Rev. **D49**, 6467 (1994); Class. Quantum Grav. **15**, 3147 (1998); Phys. Rev. **70**, 104027 (2004); Phys. Rev. Lett. **93**, 251101 (2004).
[35] A. Ashtekar and B. Krishnan, Phys. Rev. Lett. **89**, 261101 (2002); Phys. Rev. **D68**, 104030 (2003).
[36] W. A. Hiscock, Phys. Rev. **D23**, 2813; 2823 (1981).